High-Precision Shock Wave Measurements of Deuterium: Evaluation of Exchange-Correlation Functionals at the Molecular-to-Atomic Transition

M. D. Knudson[1,2] and M. P. Desjarlais[1]
[1]Sandia National Laboratories, Albuquerque, New Mexico 87185, USA
[2]Institute for Shock Physics, Washington State University, Pullman, Washington 99164-2814, USA
(Received 12 August 2016; revised manuscript received 3 October 2016; published 20 January 2017)

We present shock compression data for deuterium through the molecular-to-atomic transition along the principal Hugoniot with unprecedented precision, enabling discrimination between subtle differences in first-principle theoretical predictions. These observations, supported through reshock measurements, provide tight constraints in a regime directly relevant to planetary interiors. Our findings are in best agreement with density functional theory; however, no one exchange-correlation functional describes well both the onset of dissociation and the maximum compression along the Hugoniot.

DOI: 10.1103/PhysRevLett.118.035501

The high-pressure (P) response of hydrogen and its isotopes remains a problem of broad scientific interest. The high-P equation of state of this element has significant implications for inertial confinement fusion, planetary astrophysics, and our fundamental understanding of warm dense matter. In particular, hydrogen, as one of the simplest elemental systems, has been a model system in the development of advanced first-principle simulation techniques including finite temperature density functional theory (FT-DFT) and quantum Monte Carlo (QMC) methods [1]. Dynamic compression of deuterium through shock wave experiments has been paramount in guiding our understanding of the high-P response of this element, and in the evaluation of emerging computational techniques.

Previous experimental studies have provided data along the principal Hugoniot—the locus of end states achievable through compression by large amplitude shock waves—through gas-gun [2], laser-driven [3,4], explosively driven [5], and magnetically driven experiments [6] (see Fig. S-5 of Ref. [7]). However, these difficult experiments have been limited in accuracy, largely because the relatively low impedance of deuterium requires accurate knowledge of the deep release of the experimental standard used in the measurements. While these measurements have constrained the maximum compression on the Hugoniot through the molecular-to-atomic (MA) transition to be ~four–to fivefold, to date the precision of these measurements has not been sufficient to confidently distinguish the fidelity of various first-principle simulation methods.

We present the results of magnetically accelerated flyer plate experiments on deuterium using α-quartz as an impedance matching standard, taking advantage of recent high-precision Hugoniot measurements [11] and an experimentally determined release model [12] for α-quartz. These results, with an unprecedented precision of ~1.5%–1.9% in density along the deuterium Hugoniot, are corroborated through reshock measurements from these Hugoniot states that provide off-Hugoniot data in the ~100–200 GPa and ~5–15 kK regime that are directly relevant to the interiors of gas giant planets [13]. Combined, the Hugoniot and reshock measurements provide stringent constraints on the behavior of deuterium in the vicinity of the MA transition, and allow for high fidelity comparison with first-principle simulation methods.

These results are found to be in disagreement with recent computational results using QMC methods [14], and are currently better described by FT-DFT. Motivated by favorable comparisons between nonlocal exchange-correlation (xc) functionals with the recent observation of the MA transition of deuterium in the low temperature regime [15], we compared these experimental results with optB86b [16], vdW-DF1 [17], and vdW-DF2 [18] in addition to PBE [19]. We found good agreement for the onset of the MA transition with the vdW xc functionals, and in particular vdW-DF1. However, peak compression along the Hugoniot was found to be higher than that predicted by vdW-DF1 and in better agreement with PBE, suggesting the P range over which dissociation occurs on the Hugoniot is overestimated by the vdW xc functionals. These insights into the shortcomings of current first-principle theory should aid in future theoretical efforts and the development of new xc functionals.

A series of experiments on deuterium was performed on the Sandia National Laboratories' Z machine [20], a pulsed power accelerator capable of producing extremely large current (~20 MA) and magnetic field densities (~10 MG) within a short-circuit, coaxial load geometry. These current and magnetic field densities result in substantial magnetic pressures (in excess of 400 GPa) produced over time scales of a few hundred nanoseconds. The resulting impulse propels the outer anode plates of a coaxial load outward at high velocity, capable of being used in high-precision

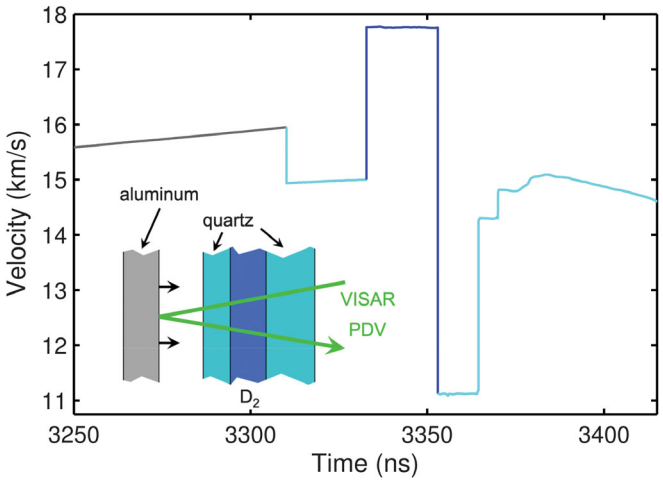

FIG. 1. Representative experimental data, in this case from VISAR. Gray line: aluminum flyer plate velocity. Cyan (blue) line: α-quartz (deuterium) shock velocity. The inset shows a schematic of the experimental configuration; note the dimensions are not to scale.

equation of state measurements in the multimegabar regime [21,22]. For this study, 17×40 mm aluminum flyer plates were magnetically accelerated to peak velocities between ~15 and 29 km/s.

The flyer plate impacted a cryocell consisting of α-quartz front and rear windows (300 and 1500 μm, respectively) contained within a copper body. A liquid deuterium sample (~300 μm) was created by condensing high purity deuterium gas (held at 18 psi) in the cryocell using a disposable cryostat [23]. A resistive heater, controlled by a temperature sensor in a feedback loop, was used to maintain a temperature of 22.0 ± 0.1 K, producing a quiescent liquid sample with a nominal initial density of 0.167 g/cm^3 ($\pm$0.4%).

The flyer plates and cryocell were diagnosed using velocity interferometry; measurements were made using both the Velocity Interferometer System for Any Reflector (VISAR [24]) and Photonic Doppler Velocimetry (PDV [25]). Since all of the materials are transparent, the 532-nm (VISAR) and 1550-nm (PDV) lasers could pass through the cryocell and reflect off the flyer plate surface, as illustrated in the inset of Fig. 1. This allowed measurement of the flyer plate velocity from initial motion to impact, along with direct measurement of the shock velocities in α-quartz and deuterium, both of which become reflective in this P regime.

The measured apparent velocity v_a must be reduced by a factor equal to the refractive index of the unshocked material to obtain the actual velocity: $v = v_a/n_0$. The values of n_0 used for α-quartz and deuterium were 1.547 (1.528) and 1.133 (1.124) at 532 (1550) nm, respectively [26,27]. Ambiguity in the fringe shift upon both impact and transition of the shock velocity measurement from α-quartz to deuterium was mitigated through the use of three different VISAR sensitivities, or velocity per fringe settings, at each measurement location (including a high-sensitivity velocity per fringe setting of 0.2771 km/s per fringe). We conservatively estimate the resolution of the VISAR system at one tenth of a fringe, resulting in uncertainty in flyer plate and shock velocities of a few tenths of a percent. A representative velocity profile is shown in Fig. 1.

The shocked state of the deuterium was determined using the impedance matching technique (see Fig. S-1 of Ref. [7]) and the Rankine-Hugoniot (RH) jump relations [28]. Briefly, the shocked state of the α-quartz drive plate was determined from the known Hugoniot of α-quartz [11] and the measured shock velocity U_s^Q. Upon transmission of the shock into the deuterium, the state of the drive plate is constrained to lie on a release adiabat emanating from pressure and particle velocity (P^Q, u_p^Q); a recently developed release model [12] was used to determine the release path [7]. The shocked state of the deuterium is constrained to lie along a chord with slope given by the product of the measured shock velocity of deuterium and the known initial density: $\rho_0 U_s^D$. The intersection of these two curves provides P_1 and u_{p1}; the RH jump relations then provide the density compression (ρ_1/ρ_0) in the shocked state. Uncertainties in all kinematic values were determined through a Monte Carlo technique [29]. We emphasize that this approach ensures propagation of all random measurement errors and systematic errors in the α-quartz standard (both Hugoniot and release). The 1σ uncertainties in u_{p1}, P_1, and ρ_1/ρ_0 were found to be ~0.5%, ~0.6%, and ~1.5%–1.9%, respectively.

A total of five Hugoniot experiments were performed, one at ~140 GPa well into the fully dissociated liquid regime, and four over the range of 35 to 60 GPa in the vicinity of the MA transition and maximum compression along the principal Hugoniot. Results of these experiments are shown as the cyan symbols in Figs. 2 and 3. Also shown are Hugoniot data of Nellis *et al.* [2] and the predicted Hugoniot response from several models: Sesame72 [30], Kerley03 [31], PW91 as implemented by Lenosky *et al.* [32,33], PW91 [32,34], PBE [19], optB86b [16], vdW-DF1 [17], vdW-DF2 [18], and QMC calculations [14]. Note that a reanalysis [7] of the gas-gun data of Nellis *et al.*, using improved standards for tantalum and aluminum for impedance matching (including a recent aluminum release model [35]), resulted in a slight increase in inferred particle velocity (~0.5%–0.7%) and decrease in inferred density compression (~1%–2%) as compared to the originally published results. Also shown are reanalyzed results [7] from plate impact experiments performed at the Z facility using an aluminum standard [6]; weighted averages of these data, with up to seven individual experiments per weighted average point, are shown. Results with the two standards are found to be consistent (reduced χ-squared of 0.74 for the aluminum standard data set with respect to the quartz standard fit), lending confidence that all sources of error have been accounted for. In the subsequent evaluation of first-principle theory we choose to focus on the fit to the

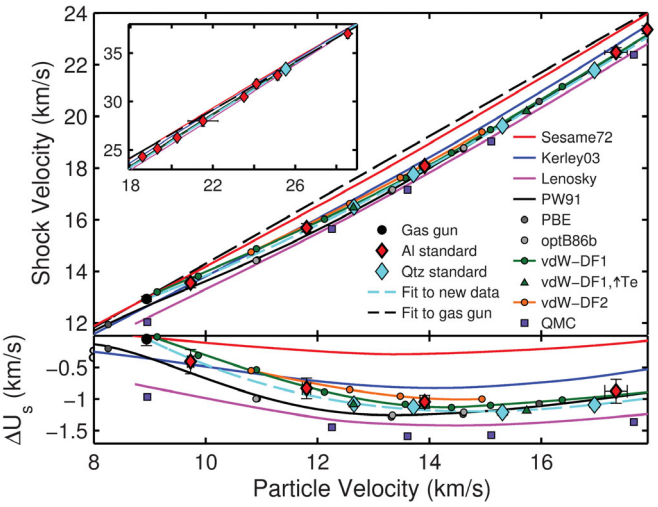

FIG. 2. Deuterium $U_s - u_p$ Hugoniot. Chemical picture models: red line, Sesame72 [30]; blue line, Kerley03 [31]. FT-DFT: magenta line, Lenosky *et al.* [33]; black line, PW91 [32,34] corrected for ρ_0 of 0.167 g/cm^3; dark gray circles, PBE, this work; light gray circles, optB86b, this work; green line, green circles, vdW-DF1, this work; green triangle, vdW-DF1 with elevated T_e, this work; orange line, orange circles, vdW-DF2, this work. QMC: purple squares, Tubman *et al.* [14]. Data: black circles, gas gun [2]; red diamonds, plate impact with aluminum standard [6], reanalyzed using the recent aluminum release model [35] (weighted averages of up to seven individual experiments); cyan diamonds, plate impact with α-quartz standard, this work. Dashed black line, extrapolation of the weighted least-squares linear fit to the gas-gun data [2]; dashed cyan line, weighted least-squares piecewise fit to the experimental data shown here. The lower panel plots ΔU_s relative to the fit to the gas-gun data (dashed black line).

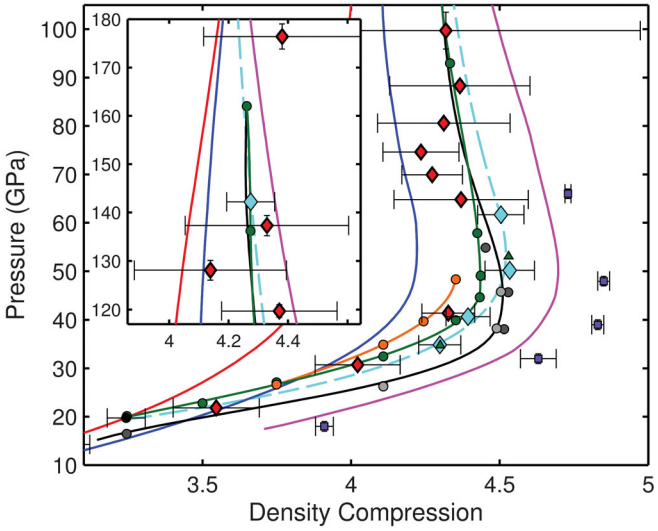

FIG. 3. Deuterium P-density compression Hugoniot (all relative to $\rho_0 = 0.167$ g/cm^3). Lines and symbols are as in Fig. 2. Note that the x and y scales of the inset match the main figure.

quartz standard data, as the quartz standard provides a more constraining measurement [7].

Through the MA transition the effects of dissociation are manifest by a transient drop in the slope of U_s relative to u_p, resulting in an increase in ρ_1/ρ_0 as energy goes into the breaking of bonds. This is best illustrated in the lower panel of Fig. 2, which shows the difference in U_s with respect to the extrapolated fit to the gas-gun data of Nellis *et al.* [2]. The onset of the drop in slope is coincident with the onset of dissociation, while the magnitude of the difference dictates the maximum compression along the Hugoniot. Both the Lenosky *et al.* [33] and recent QMC [14] results exhibit too large a drop that begins at much too low P. In the case of Lenosky *et al.* this was shown to be due to inadequate convergence (particularly in P) and omission of zero-point energy in the initial energy state [34]; increased energy cutoffs and inclusion of zero-point energy in the initial state result in an increase in P for the onset of dissociation and significantly lower density compression through the MA transition (PW91 in Figs. 2 and 3), in better agreement with both the gas-gun and the Z results. The similarity between the Lenosky *et al.* and QMC results raises questions concerning the level of convergence and the small system size in the recent QMC results.

In comparison with these new Hugoniot measurements, however, PW91 still shows signs of dissociation at too low P. Recent experimental work on the low-temperature metallization of deuterium [15] suggests an improved description of the MA transition by xc functionals that account for van der Waals interactions. This prompted the evaluation of several nonlocal xc functionals along the Hugoniot near the MA transition, including optB86b [16], vdW-DF1 [17], and vdW-DF2 [18]. Calculations were performed using version 5.3 of VASP [36]. Coulomb interactions between the electrons and ions were treated using projector-augmented wave potentials [37]. For consistency, all calculations performed for this study [7] (including new PBE [19] calculations) included 128 atoms in the supercell, plane wave cutoff energies of 1200 eV, Baldereschi's mean value point for the **k**-point spectrum, and ρ_0 of 0.167 g/cm^3 (prior PW91 calculations [34] were at ρ_0 of 0.171 g/cm^3 and here are corrected for the lower ρ_0). We also investigated the importance of nuclear quantum effects [7] at the lowest P considered here (~20 GPa) through path integral molecular dynamics; for vdW-DF1 at the same ρ_1/ρ_0 path integral molecular dynamics predicted a slightly lower P (0.6 GPa) and T (208 K). These differences would be even smaller at higher P and T along the Hugoniot. Additional details, including a discussion of the uncertainties associated with FT-DFT calculations, can be found in the Supplemental Material [7].

Evaluation of the various xc functionals were made quantitative by comparing fits to the various xc functional results and experiment. As seen in Figs. 2 and 3, the observed shifts in the drop in slope of U_s correspond to P shifts (with respect to the experimental fit) on the order of ~1 GPa higher

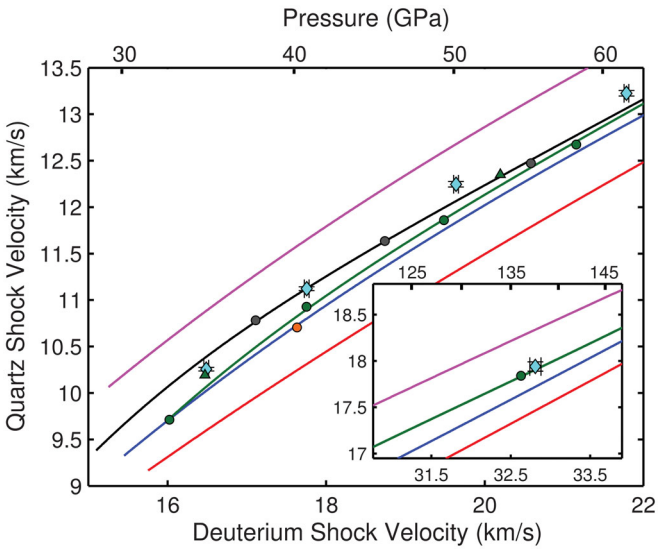

FIG. 4. Deuterium reshock experimental observables: U_s^Q vs U_s^D. Lines and symbols are as in Fig. 2. Note that the x and y scales of the inset match the main figure.

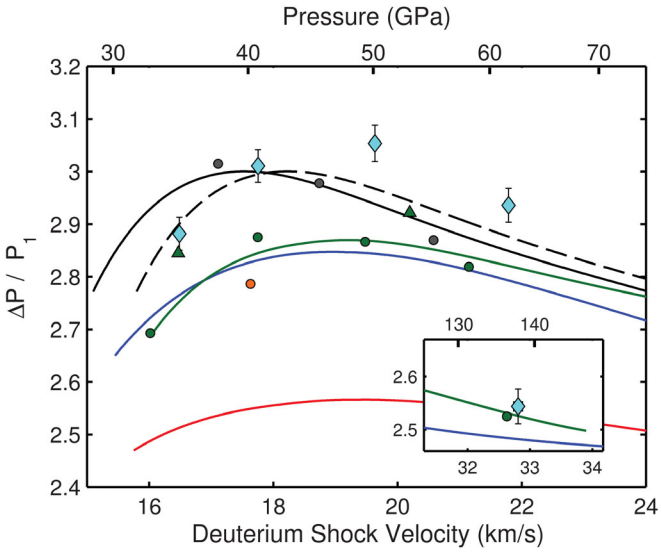

FIG. 5. Ratio of the increase in P upon reshock to first shock pressure ($\Delta P/P_1$) as a function of P_1 for reshock from an α-quartz anvil. Lines and symbols are as in Fig. 2. The dashed black line is the PW91 result shifted ~3 GPa to higher P. Note that the x and y scales of the inset match the main figure.

for vdW-DF1 and vdW-DF2, ~3 GPa lower for PW91, PBE, and optB86b, and ~10 GPa lower for the recent QMC calculations. Thus, it appears that the experimentally observed onset of dissociation is bounded below by PW91, PBE, and optB86b, and above by vdW-DF1 and vdW-DF2. Peak compression along the Hugoniot was found to be overestimated (~7%) by QMC calculations, underestimated (~2%–4%) by the vdW-DF xc functionals, and reasonably well described by PW91 and PBE, albeit with the experimentally observed peak compression occurring at somewhat higher P (similar to the onset of dissociation).

These conclusions are also supported by the reshock data from the present experiments. In all five of the Hugoniot experiments described above, the reflected shock from the rear α-quartz window drove the deuterium from the Hugoniot state to a reshocked state at higher P and ρ. The observables for these reshock experiments, the measured shock velocity in the deuterium immediately prior to reflection from the rear α-quartz window, U_s^D, and the measured shock velocity in the rear α-quartz window, U_s^Q, are shown in Fig. 4. Also shown in the figure are predictions for a subset of the models; impedance matching was performed to determine the expected U_s^Q for a given U_s^D for each model [7]. At higher P (~140 GPa), well into the fully dissociated liquid regime, the reshock is well described by vdW-DF1. However, in the vicinity of the MA transition differences are observed between the various xc functionals and experiment, with the differences following the trend with compressibility—the more compressible models on the principal Hugoniot exhibit a higher reshock P, and thus U_s^Q.

This trend with first shock compressibility can be made quantitative by considering the ratio of the increase in P upon reshock to the first shock pressure: $\Delta P/P_1 = (P_2 - P_1)/P_1$, as shown in Fig. 5. Evaluation of this ratio with the RH jump relations [7] shows that this quantity is quite sensitive to density compression along the principal Hugoniot. As was the case for the principal Hugoniot, the onset of dissociation (here manifest by a rapid increase in $\Delta P/P_1$) appears to occur at too low P for PW91 and PBE. The onset of the MA transition is better described by vdW-DF1; however, the first shock compressibility is too low. In contrast, the peak compressibility is better described by PW91 and PBE; in particular the experimental observations are reasonably reproduced by PW91 with a ~3 GPa shift to higher P (dashed black line in Fig. 5), consistent with conclusions inferred from the principal Hugoniot comparison.

The difference in the peak compression between vdW-DF1 and PBE is likely related to the P width over which dissociation occurs along the principal Hugoniot. Examination of the peak in the pair correlation function [7] (as an indicator of the extent of bonding) suggests that in addition to delaying the onset of dissociation with respect to PBE, vdW-DF1 also predicts a significantly wider P range for dissociation to complete (~30% wider than PBE [7]). This results in a first shock compressibility that is too low near peak compression for vdW-DF1. It also results in a higher reshock compressibility in this P regime [see Figs. S-2(b) and S-6 of Ref. [7]], as energy is continuing to go into the breaking of bonds.

To test this hypothesis we performed vdW-DF1 calculations at elevated electron temperature (T_e) [7]. The effect of the elevated T_e was to weaken the molecular bonds, resulting in a narrower P range over which dissociation takes place along the Hugoniot (see Fig. S-7 of Ref. [7]). As seen in Figs. 2–5, these elevated T_e calculations (dark green

triangles) also exhibited an increased compressibility along the Hugoniot, a higher U_s^Q for a given U_s^D, and a higher $\Delta P/P_1$, all in better agreement with the experimental observables. The insight gained from these measurements provides a much needed benchmark for theory and a means for evaluation of future theoretical developments (i.e., QMC calculations) and new xc functionals.

In conclusion, we have performed Hugoniot and reshock experiments on deuterium in the vicinity of the MA transition with unprecedented precision. These measurements, which allow for high fidelity comparison with first-principle theory, are in disagreement with recent QMC calculations and suggest the MA transition along the Hugoniot is currently better described by FT-DFT. However, no one xc functional completely describes all experimental observables. While the onset of the MA transition is best described by vdW-DF1, the P width over which dissociation occurs is likely overestimated by vdW-DF1, and is in better agreement with PBE. These results provide an important benchmark for first-principle theory, a means for evaluation of future theoretical developments and new xc functionals, and stringent constraints on the high-P response of hydrogen in a regime that is directly relevant to planetary interiors.

We acknowledge the crew of the Sandia Z facility for their contributions to these experiments. Sandia National Laboratories is a multiprogram laboratory managed and operated by Sandia Corporation, a wholly owned subsidiary of Lockheed Martin Corporation, for the U.S. Department of Energy's National Nuclear Security Administration under Contract No. DE-AC04-94AL85000.

[1] J. M. McMahon, M. A. Morales, C. Pierleoni, and D. M. Ceperley, Rev. Mod. Phys. **84**, 1607 (2012).
[2] W. J. Nellis, A. C. Mitchell, M. van Thiel, G. J. Devine, R. J. Trainor, and N. Brown, J. Chem. Phys. **79**, 1480 (1983).
[3] D. G. Hicks, T. R. Boehly, P. M. Celliers, J. H. Eggert, S. J. Moon, D. D. Meyerhofer, and G. W. Collins, Phys. Rev. B **79**, 014112 (2009).
[4] P. Loubeyre, S. Brygoo, J. Eggert, P. M. Celliers, D. K. Spaulding, J. R. Rygg, T. R. Boehly, G. W. Collins, and R. Jeanloz, Phys. Rev. B **86**, 144115 (2012).
[5] G. V. Boriskov, A. I. Bykov, R. I. Il'kaev, V. D. Selemir, G. V. Simakov, R. F. Trunin, V. D. Urlin, A. N. Shuikin, and W. J. Nellis, Phys. Rev. B **71**, 092104 (2005).
[6] M. D. Knudson, D. L. Hanson, J. E. Bailey, C. A. Hall, J. R. Asay, and C. Deeney, Phys. Rev. B **69**, 144209 (2004).
[7] See Supplemental Material at http://link.aps.org/supplemental/10.1103/PhysRevLett.118.035501, which includes Refs. [8–10], for (i) more details regarding the experimental setup and analysis, (ii) a slight revision to the quartz and aluminum release models, (iii) reanalysis of previous experimental results that used an aluminum standard, and (iv) more details regarding the first-principle calculations performed as a part of this study.
[8] S. Root, T. R. Mattsson, K. R. Cochrane, R. W. Lemke, and M. D. Knudson, J. Appl. Phys. **118**, 205901 (2015).
[9] S. Root (unpublished).
[10] R. C. Clay III, J. Mcminis, J. M. McMahon, C. Pierleoni, D. M. Ceperley, and M. A. Morales, Phys. Rev. B **89**, 184106 (2014).
[11] M. D. Knudson and M. P. Desjarlais, Phys. Rev. Lett. **103**, 225501 (2009).
[12] M. D. Knudson and M. P. Desjarlais, Phys. Rev. B **88**, 184107 (2013).
[13] N. Nettelmann, R. Püstow, and R. Redmer, Icarus **225**, 548 (2013).
[14] N. M. Tubman, E. Liberatore, C. Pierleoni, M. Holzmann, and D. M. Ceperley, Phys. Rev. Lett. **115**, 045301 (2015).
[15] M. D. Knudson, M. P. Desjarlais, A. Becker, R. W. Lemke, K. R. Cochrane, M. E. Savage, D. E. Bliss, T. R. Mattsson, and R. Redmer, Science **348**, 1455 (2015).
[16] J. Klimeš, D. R. Bowler, and A. Michaelides, J. Phys. Condens. Matter **22**, 022201 (2010).
[17] M. Dion, H. Rydberg, E. Schröder, D. C. Langreth, and B. I. Lundqvist, Phys. Rev. Lett. **92**, 246401 (2004).
[18] K. Lee, E. D. Murray, L. Kong, B. I. Lundqvist, and D. C. Langreth, Phys. Rev. B **82**, 081101 (2010).
[19] J. P. Perdew, K. Burke, and M. Ernzerhof, Phys. Rev. Lett. **77**, 3865 (1996).
[20] M. Matzen, M. A. Sweeney *et al.*, Phys. Plasmas **12**, 055503 (2005).
[21] R. Lemke, M. D. Knudson, A. Robinson, T. Haill, K. Struve, J. Asay, and T. Mehlhorn, Phys. Plasmas **10**, 1867 (2003).
[22] R. Lemke, M. D. Knudson, and J.-P. Davis, Int. J. Impact Eng. **38**, 480 (2011).
[23] S. Root, K. R. Cochrane, J. H. Carpenter, and T. R. Mattsson, Phys. Rev. B **87**, 224102 (2013).
[24] L. M. Barker and R. E. Hollenbach, J. Appl. Phys. **43**, 4669 (1972).
[25] O. T. Strand, D. R. Goodman, C. Martinez, T. L. Whitworth, and W. W. Kuhlow, Rev. Sci. Instrum. **77**, 083108 (2006).
[26] G. Ghosh, Opt. Commun. **163**, 95 (1999).
[27] P. C. Souers, *Hydrogen Properties for Fusion Energy* (University of California Press, Berkeley, 1986).
[28] G. E. Duvall and R. A. Graham, Rev. Mod. Phys. **49**, 523 (1977).
[29] M. D. Knudson, M. P. Desjarlais, R. W. Lemke, T. R. Mattsson, M. French, N. Nettelmann, and R. Redmer, Phys. Rev. Lett. **108**, 091102 (2012).
[30] G. I. Kerley, Phys. Earth Planet. Inter. **6**, 78 (1972).
[31] G. Kerley, Technical Report No. SAND2003-3613, Sandia National Laboratories, 2003.
[32] Y. Wang and J. P. Perdew, Phys. Rev. B **44**, 13298 (1991).
[33] T. J. Lenosky, S. R. Bickham, J. D. Kress, and L. A. Collins, Phys. Rev. B **61**, 1 (2000).
[34] M. P. Desjarlais, Phys. Rev. B **68**, 064204 (2003).
[35] M. D. Knudson, M. P. Desjarlais, and A. Pribram-Jones, Phys. Rev. B **91**, 224105 (2015).
[36] G. Kresse and J. Furthmüller, Phys. Rev. B **54**, 11169 (1996).
[37] G. Kresse and D. Joubert, Phys. Rev. B **59**, 1758 (1999).